Throughput Analysis between Unicast and MBSFN from Link Level to System Level

Chunmei Liu*, Chen Shen†, Jack Chuang*, Richard A. Rouil*, and Hyeong-Ah Choi†
*Wireless Networks Division, National Institute of Standards and Technology, USA
†Department of Computer Science, George Washington University, USA
Email: *{chunmei.liu, jack.chaung, richard.rouil}@nist.gov, †{shenchen, hchoi}@gwu.edu

***Abstract*—Public safety incidents typically involve significant amount of group traffic. This paper initializes our study in exploring the potential spectrum savings and improvement in first responders experience by using Multicast Broadcast Single Frequency Network (MBSFN) to serve group traffic among first responders. Towards this goal, this paper proposes a comprehensive methodology that closely follows The 3rd Generation Partnership Project (3GPP) specifications and considers unicast multiple-input multiple-output (MIMO) and MBSFN without MIMO. High fidelity Block Error Rate (BLER) curves for both MBSFN and unicast are generated, and Signal-to-noise ratio (SNR) points to switch Channel Quality Indicators (CQIs) are extracted and analyzed. Several simulation scenarios have been designed and the empirical results are analyzed.**

***Index Terms*—BLER curves, CQI, LTE, MBSFN, MIMO, public safety broadband network, unicast.**

I. Introduction

In 2012, the Congress passed the Middle Class Tax Relief and Job Creation Act of 2012 [1]. The act calls for the establishment of a national public safety broadband network to expand high-speed wireless broadband and to improve communications interoperability among first responders. Meanwhile, the Long Term Evolution (LTE) networks have been deployed for several years throughout the nation to serve millions of commercial users, and point-to-point unicast transmission is the typical mechanism deployed.

Compared with commercial traffic, public safety incidents typically involve significant amount of group traffic among first responders [2]. Using traditional point-to-point unicast communication to serve this traffic requires to transmit the same content multiple times over the air interface. On the contrary, if multicast transmission is used, the content needs to be transmitted only once over the air interface. This potential saving on the precious spectrum and improvement in first responders' user experience trigger the exploration of using multicast to serve group traffic among first responders. Towards this goal, this paper considers the public safety broadband network that is currently built upon LTE technologies using Band 14 (B14) 10 MHz bandwidth Frequency Division Duplex (FDD), with focus on downlink and Multimedia Broadcast Multicast Service Single Frequency Network (MBSFN) [3].

MBSFN has been studied in the literature from various perspectives. In [4], four adaptive Modulation and Coding Scheme (MCS) selection algorithms have been proposed. Except the bottom-up algorithm which selects the minimum MCS for all user equipments (UEs) in MBSFN, the others cannot guarantee all UEs to successfully decode the data. Also this work directly uses unicast Block Error Rate (BLER) curves for MBSFN. In [5], MBSFN and Single Cell Point To Multipoint (SC-PTM) are evaluated together with the unicast transmission. However, an important feature, multiple-input multiple-output (MIMO), is not considered in unicast. In [6], an optimal UE grouping algorithms in MBSFN is proposed. Since the minimum MCS is selected for all UEs in MBSFN, UE grouping with separate assigned resource may improve the overall performance. There the UE is associated with the same MCS in unicast and multicast modes. As we will see later, it is not always the case. The performance of Multimedia Broadcast Multicast Services (MBMS) and unicast when transmitting video is compared in [7]. The authors use average MCS of all UEs for the expected performance calculation. The comparison is also based on the same MCSs for unicast and multicast.

Our ultimate goal is to quantify network and user performance improvements if MBSFN and unicast communications are adapted based on specific network deployments and device distributions. Our system model and simulation closely follow the 3rd Generation Partnership Project (3GPP) standard with MIMO features included for unicast transmission but not MBSFN [3] [8]. Signal-to-interference-plus-noise ratio (SINR) values in unicast and MBSFN are calculated separately based on their unique models, thus we do not simply use MCS in unicast settings for the MBSFN. In addition, by considering comprehensive physical (PHY) and medium access control (MAC) layers, link level simulations were conducted and traceable high fidelity BLER vs Signal-to-Noise Ratio (SNR) vs Channel Quality Indicator (CQI) curves were generated and analyzed. To our knowledge, this modeling with the above features together for system level performance analysis is the first of its kind.

The rest of this paper is organized as follows. Section II reviews MBSFN and unicast as defined in 3GPP. Section III outlines our methodology and describes our link level simulation design in detail. Simulation results and analysis are presented and summarized in Section IV. Finally, Section V summarizes the paper and outlines steps for future research.

II. Review of unicast and MBSFN in 3GPP

With focus on major factors that have direct impacts on performance comparison and simulation design, this section

reviews MBSFN as specified by 3GPP, and highlights differences between unicast and MBSFN.

In MBSFN, MBMS data is transmitted from multiple cells to the destination UE. All cells involved are tightly synchronized and transmit the same content over the same subcarriers, and all transmissions received by the UE differ only in arrival times, amplitudes, and phases. Given the redundant transmissions via multiple eNodeBs, the SINR is improved, with the greatest improvement being seen at the cell edge.

Fig. 1 illustrates a typical MBSFN subframe as specified in 3GPP [9], with one subframe lasting one Transmission Time Interval (TTI) in time domain. The non-MBSFN region is for controls and signals, and the MBSFN region is where MBMS data is transmitted. In the MBSFN region, in addition to MBMS data, MBSFN reference signals (RSs) are used by the UEs for channel estimation. Note that there is a gap between the two regions [9].

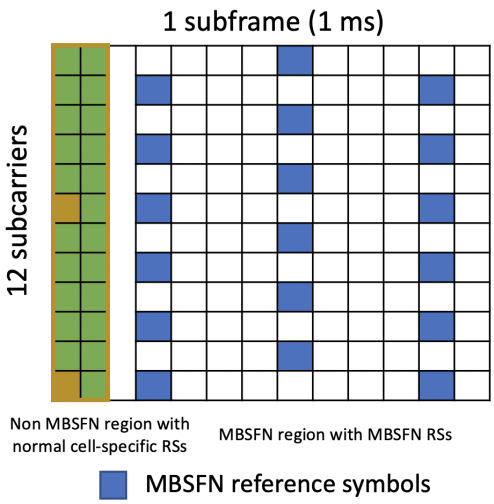

Fig. 1: MBSFN Subframe Structure

As a comparison, Fig. 2 illustrates a typical unicast subframe. The figure shows the configuration with normal cyclic prefix (CP) and 2 symbols for control region, which are typical LTE network settings. The cell-specific reference signals (CRSs) shown are with one antenna port. Subframe structure with other configurations can be found in [9].

By comparing Fig. 1 and Fig. 2, it can be seen that MBSFN RSs have tighter spacing than unicast CRSs, which leads to higher overhead and less resource elements (REs) available for user data transmissions. In addition, MBSFN subframes and non-MBSFN subframes are interleaved in time. Moreover, while normal CP is used in typical LTE networks for unicast, extended CP is used for MBSFN to facilitate transmissions from multiple cells to arrive at the UE within CP. This reduces the number of OFDM symbols available for user data from 12 for unicast to 10 for MBSFN, as shown in Fig. 1 and Fig. 2. Furthermore, since subframe 0, 4, 5, and 9 in each radio frame carries signals that are essential for network operations in their data region [9], these four subframes are reserved for unicast transmission and cannot be configured as MBSFN subframes.

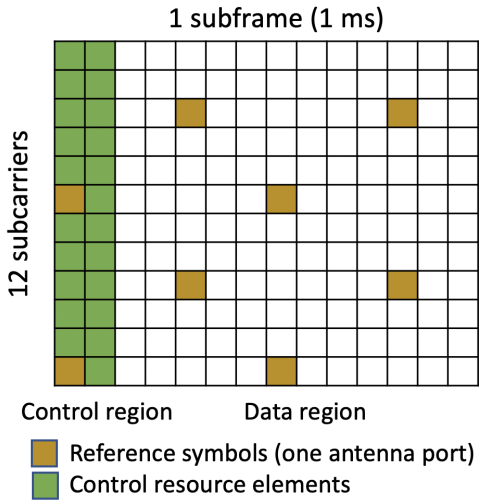

Fig. 2: Unicast Subframe Structure - One Antenna Port

3GPP also specifies that a single transport block (TB) is used per subframe for MBSFN, and that TB uses all the MBSFN resources in that subframe [3]. Specific to the public safety broadband network on B14 with 10 MHz spectrum, this corresponds to 50 resource blocks (RBs). Whereas in unicast, RBs in one subframe are typically divided into multiple sets, with each set assigned to a different user.

For unicast, MIMO has been one major technology adopted by LTE and provides significant improvements in performance and spectral efficiency. Up to release 15, 3GPP defines 10 transmission modes that are intended to fully utilize MIMO under different situations [8]. Up to two codewords can be used for a single UE. Contrarily, in MBSFN, due to its multicast nature, 3GPP specifies no transmit diversity scheme, and MBSFN is mapped on a single layer spatial multiplexing. That is, MBSFN cannot take advantage of MIMO gains.

In addition, hybrid automatic repeat request (HARQ) is a key component that ensures reliability and performance for unicast. In MBSFN, 3GPP specifies that a single transmission is used, and there is no Radio link control (RLC) retransmissions and no HARQ. Hence in order to deliver acceptable service to upper layers, lower target BLER for single transmission is typically used for MBSFN. Lost MBMS packets for certain UEs are typically recovered by retransmissions from the application layer via unicast.

III. Methodology

This section outlines the overall design for performance comparison between unicast and MBSFN, then describes the link level simulation design in detail.

A. System Model

Fig. 3 illustrates our system design. After setting up the scenario to be simulated, both unicast and MBSFN are run, and the resulting performance is recorded and compared. For both unicast and MBSFN, without loss of generality, perfect channel knowledge and zero feedback delay are assumed.

The control signaling is not modelled. For MBSFN, the unicast traffic used for application layer retransmissions are not modelled.

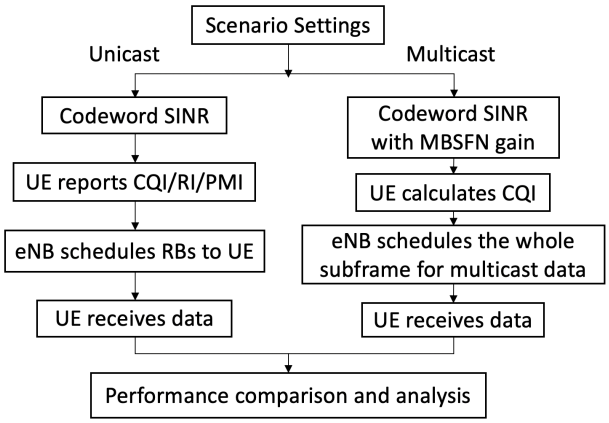

Fig. 3: Overall Design

For both unicast and MBSFN, due to its reputation of accurately predicting BLER [10]–[12], Mutual Information based Exponential SNR Mapping (MIESM) is applied to map the post-equalization SINR to Additive white Gaussian noise (AWGN) equivalent effective SNR. The general equation of the SINR to SNR mapping is as below:

$$\beta_m = f_m^{-1}\Big(\frac{1}{N_{RE}}\sum_{c=1}^{N_{RE}} f_m(\beta^c)\Big) \tag{1}$$

where β_m is the AWGN equivalent SNR for modulation m, $f_m(.)$ is the Bit Interleaved Coded Modulation (BICM) capacity of modulation alphabet m that is associated with the MCS m, β^c is the post equalization SINR for RE c, and N_{RE} is the total number of REs utilized for the transmission. In our simulation, to save simulation time, the averaging is from half RB to codeword [8].

By using Eq. (1), we can translate any channel-interference scenario to an equivalent AWGN channel, and the sample based simulation is required only once when acquiring BLER vs SNR vs CQI curves, which will be described in detail in Section III-B.

For unicast, the overall channel consists of the precomputed pathloss, shadowing, and microscale fading. The post-equalization SINR is calculated using zero forcing equalizer. Then the MIESM maps the time-frequency selective channel experienced over a number of REs and over spatial streams when spatial multiplexing is employed, to an AWGN channel that achieves the same average spectral efficiency in terms of the BICM capacity. Next, based on the AWGN BLER curves from link level simulation, each UE estimates the achievable throughput for all possible number of layers, and selects the optimal Rank Indicator (RI). Afterwards, each UE reports the selected CQI, RI, and Precoding Matrix Indicator (PMI) to the eNodeB. With the above reports from the UEs, the eNodeB schedules its RBs based on the configured scheduler, where proportional fairness scheduler is selected for our study. Finally, with the BLER curves, post-equalization SINR, and the assigned MCS from the eNodeB, each UE records successful packets and sends NACK for unsuccessful packets.

For MBSFN, the channel model used is the same as the unicast one. While calculating the post-equalization SINR, we use run time precoding and Zero-Forcing equalizer, with the modelled constructive signals from eNodeBs in the MBSFN area. The detailed modeling will be explained in [13]. The resulting post equalization SINR for RE c, β^c, can be calculated as in Eq. (2) and (3), where I_M represents the inter-symbol interference from cells that participate MBSFN transmission.

$$\beta^c = \frac{1}{\sum_{i=1}^{N_M}(1-w_i)P_i^c\|F^cH^{ic}\underline{1}_{nTx}\|^2 + I_M + \|F^c\|^2N_0} \tag{2}$$

$$I_M = \sum_{i=N_M+1}^{N} P_i^c\|F^cH^{ic}W^{ic}\|^2 \tag{3}$$

where N is the total number of cells, and the first N_M cells are those that participate in MBSFN transmission, and cell $N_{M+1}, ..., N$ are cells that do not participate in MBSFN transmission. w_i is the weighting function for cell i as defined in [14]. $P_i^c, i = 1, ..., N$ is the signal power from cell i at RE c after taking into account path loss and shadowing but without microscale fading. $H^{ic}, i = 1, ...N$ is the channel matrix from cell i to the UE at RE c. W^{ic} is the precoding matrix used by cell $i, i = N_M + 1, ..., N$. F^c is the zero-forcing equalizer. N_0 is the thermal noise. $\underline{1}_{nTx}$ is (nTx)x1 column vector with all elements being 1.

The MIESM approach is then applied to map the post equalization SINR to AWGN equivalent SNR, and each UE calculates it CQI with the MBSFN BLER curve from link level simulation (Section III-B) and reports it back to the eNodeB. The MBSFN eNodeBs select the MCS based on the minimum CQI among all MBSFN UEs and assign the whole subframe for multicast data. At last, UEs receive the data and calculate their throughput.

B. Link Level Simulation Design

As mentioned in Section III-A, the objectives of the link level simulation are to generate BLER curves for each CQI under AWGN channel, for both unicast and MBSFN, and to retrieve CQI switching points associated with target BLERs. For this purpose, Vienna link level simulator [10][1] is selected as the base platform. The simulator is designed for unicast. Its PHY layer architecture is consistent with the typical LTE physical layer procedure and that defined in 3GPP [9]. After evaluation, our simulation reused the simulator for unicast with little modifications on settings. For MBSFN, the simulator is extended to support MBSFN.

Specifically, the link simulated for both unicast and multicast is one point-to-point link between one eNB and one

[1]Any mention of commercial products in the paper is for information only; it does not imply recommendation or endorsement by NIST.

UE, with public safety band downlink center frequency of 763 MHz and 10 MHz bandwidth. CQI indices are the ones based on QPSK, 16QAM, and 64QAM, as shown in Table 7.2.3-1 in [8]. AWGN channel is chosen as mentioned in Section III-A. At the UE side, perfect channel knowledge is assumed and zero-forcing equalizer is employed. At the eNB side, transport block size (TBS) is calculated based on MCS order, coding rate, and RBs allocated as in Table 7.2.3-1 in [8]. In addition, in case of large TBS, TB segmentation and de-segmentation are performed to fit the maximum code block size defined per 3GPP [15]. Moreover, since the BLER curve is to be used in later system level simulation (Section III-A), there is no HARQ retransmission in link level simulation.

For unicast, normal CP is selected, and number of OFDM symbols for control region is set to be 2, both of which are typical LTE network deployment settings (Fig 2). Since the focus is on user data transmissions, control region is not simulated. However, since primary and secondary synchronization signal (PSS and SSS) fall into data region and occupy resource elements (REs), they are both simulated (Section II). Regarding CRSs, different RS sets map to different antenna ports [9]. To reduce the number of BLER curves used in later system level simulations and without loss of generality, RSs mapping to one antenna port is selected for this study (Fig. 2).

Per 3GPP standards, for unicast, when UE reports CQI, transport block error probability should not exceed 0.1 [8]. Hence the target BLER for CQI switching is selected to be 0.1. Also note that since PSS and SSS fall into data region in subframe 0 and 5 but not in other subframes [8], the 10 subframes within one radio frame are no longer identical in the sample space. However, within one subframe, the number of REs occupied by primary and secondary synchronization signals is small compared with total number of REs, and their impacts on BLER is hence insignificant. Therefore, to simplify the design, all subframes are treated equally in BLER calculation. 5000 subframes are simulated to provide enough confidence level.

For MBSFN, extended CP is selected as specified by 3GPP [9]. Similar to unicast simulation design, since the focus is on user data transmissions, non-MBSFN region is not simulated (Fig. 1). As mentioned in Section II, subframe 0, 4, 5 and 9 cannot be used for MBSFN. Hence they do not contribute to BLER for MBSFN and therefore are not simulated. Different from unicast, there is no need to simulate PSS and SSS. This is because they fall into subframe #0 and #5, both of which can not be used as an MBSFN subframe.

Since in MBSFN there are no HARQ retransmissions and no RLC retransmissions, lower target BLER is expected and selected to be 0.01. In addition, MBSFN subframes are identical in sample space, and 5000 subframes are simulated to provide enough confidence level.

One challenge in MBSFN simulation design is the location of MBSFN RSs. As shown in Fig. 1, MBSFN RS distribution is not the same across two slots. However, Vienna link level simulator is structured in the way that a transmit signal is mapped on REs based on symmetric slots. One major function of RSs is to support channel estimation. Since our simulation converts SINR in multipath channel to equivalent SNR and perfect channel knowledge is assumed, the locations of the RSs are not expected to change the BLER results. Based on this analysis, one design to simulate the MBSFN RSs is to simulate them by their total number instead of actual locations in subframes. We tested this design by comparing BLER curves of 16 RSs, one with uniformly distributed 16 RSs across the subframe, and the other with concentrating the 16 RSs in two OFDM symbols. The resulting BLER curves show no observable significant differences.

Based on the former analysis and verification, MBSFN RSs are simulated with focus on their total number and by putting 9 RSs at subcarrier 2 to 10 for symbol 3, and another 9 RSs at subcarrier 2 to 10 for symbol 9. Moreover, because of the assumption of perfect channel knowledge, the sequences used by MBSFN RSs would not change the simulation results. Hence, to save the effort in generating MBSFN RS sequence, the reference signal sequences Vienna generated for unicast are reused.

IV. Simulation results

Based on the simulation design described in Section III, link level simulations have been implemented and performed for the public safety band. The obtained BLER curves are shown in Fig. 4 and Fig. 5 for unicast and MBSFN, respectively. The curves in Fig. 4 and Fig. 5 successfully support our initial projection that there would be no significant difference between MBSFN and unicast BLER curves over SNR in AWGN channel, despite that the MBSFN BLER curves shift a little bit to the left. The CQI is the major parameter which will impact BLER in AWGN.

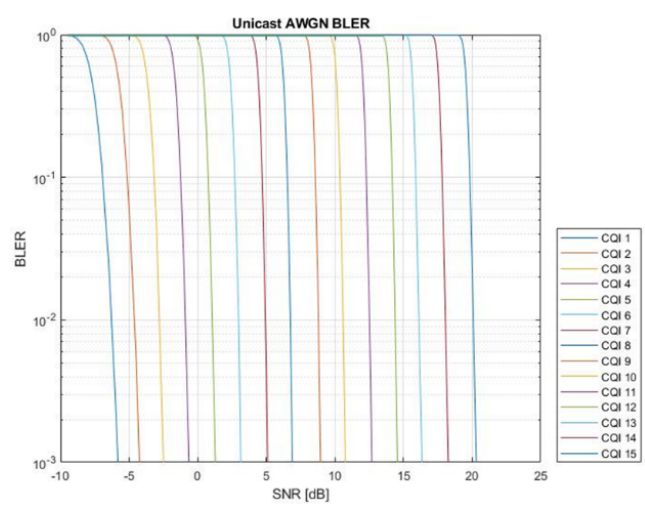

Fig. 4: Unicast BLER for AWGN B14 700 MHz Downlink

Given a target BLER of 0.1 for unicast and 0.01 for MBSFN, we also extracted CQI switching points and listed them in Table I. For comparison purposes, switching points for target BLER of 0.01 for unicast and 0.1 for MBSFN are also listed. We discovered that for the same target BLER, for

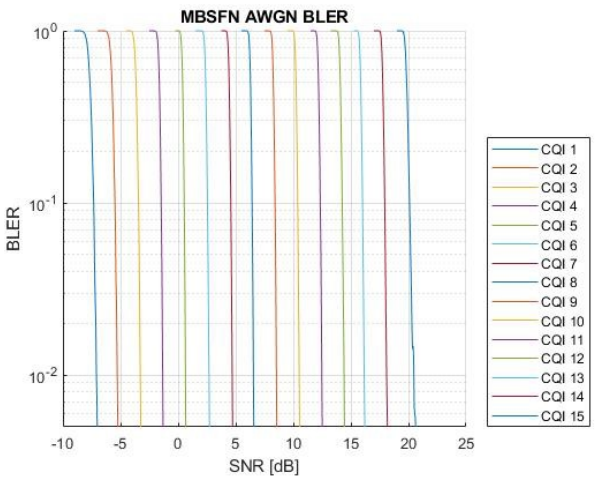

Fig. 5: MBSFN BLER for AWGN B14 700 MHz Downlink

low CQIs, MBSFN requires less SNR than unicast, while for high CQIs, unicast requires less SNR. We also discovered that with different target values, the switching points do not differ significantly.

Note that similar BLER curves and CQI switching points do not imply that the unicast and MBSFN will perform similarly in actual networks. Due to different system architecture, in actual networks when unicast or MBSFN is applied, the first responders could experience different combined SINR before the equalizer even in the same multipath scenario (for example after MBSFN gain especially at cell edge). After the SINR to SNR translation, the AWGN equivalent SNR is different. This could lead to different CQI reports for MBSFN and unicast to meet BLER requirement, and hence different performance first responders would experience. This projection is verified by the system level simulation results described below.

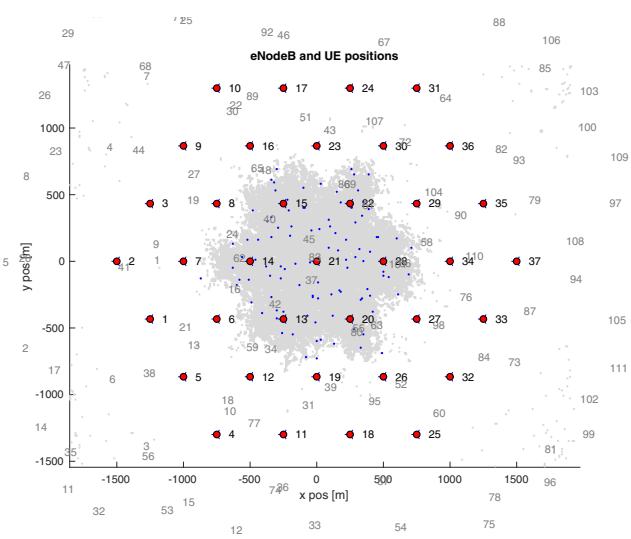

Fig. 6: Network Layout

The network layout used in the system level simulation is shown in Fig. 6. The network is the typical tri-sectored site hexagonal grid with 37 sites and 111 cells in total. First responders are uniformly located in the shaded center 7 sites 21 cells, with 5 first responders per cell unless mentioned otherwise. The outer two rings of 30 sites are included to simulate interference. Inter-site distance is set to be 500 meters. The eNB transmission power is set as 40 W, and the antenna height and the receiver height are 32 m and 1.5 m, respectively. The number of eNB transmit antennas is 8, and the number of UE receiver antennas is 4. Urban macro channel model is used [16]. For unicast, transmission mode 9 [8] is employed, which allows spatial multiplexing to take advantage of MIMO gains. For MBSFN, the MBSFN area is the center 7 sites where first responders are located.

Fig. 7 shows the cumulative distribution function (CDF) of the average AWGN equivalent effective SNR over time experienced by codewords for unicast and MBSFN. Note that in unicast when more than 1 layer is applied (MIMO), the number of codewords could be 2. In this case, the effective SNR of each codeword contributes to one sample in generating the CDF. This figure shows that MBSFN has significant higher effective SNR than unicast. This improvement comes from several factors. The first is that in unicast the cells in the center 7 sites generate interference to each other, while in MBSFN they do not. The second is the MBSFN gain due to transmissions from multiple cells. The third is that in unicast when there are two codewords, the signal power is distributed to two codewords instead of one, which lower the SNR of each codeword.

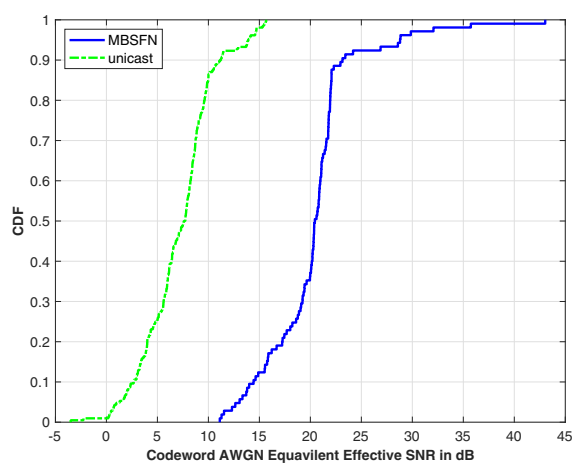

Fig. 7: CDF of AWGN Equivalent Effective SNR

Fig. 8 shows comparison of reported CQI between MBSFN and unicast from 10 randomly selected UEs in TTI 23. Note that for unicast, some UEs report 2 CQIs and some report 1. This is because with MIMO when there are two codewords, each codeword is associated with one CQI. It can be observed that in the selected case, MBSFN has higher CQI than unicast, which is consistent with Fig. 7. Contrary to the assumption in some literature which assume that MBSFN MCS is the

	CQI	1	2	3	4	5	6	7	8	9	10	11	12	13	14	15
MBSFN	target BLER 0.1	-7.3	-5.45	-3.4	-1.45	0.55	2.55	4.6	6.45	8.45	10.4	12.4	14.3	16.1	18	20.1
	target BLER 0.01	-7.05	-5.25	-3.25	-1.3	0.65	2.7	4.7	6.55	8.55	10.6	12.5	14.5	16.2	18.2	20.5
Unicast	target BLER 0.1	-6.94	-5.15	-3.18	-1.25	0.76	2.7	4.69	6.53	8.57	10.4	12.3	14.2	15.9	17.8	19.8
	target BLER 0.01	-6.29	-4.62	-2.8	-0.91	1.06	2.98	4.93	6.75	8.79	10.6	12.5	14.4	16.1	18.1	20.1

TABLE I: CQI switching points at target BLER 0.1 and 0.01, SNR in dB

minimum of unicast MCSs of all UEs, the lowest MBSFN CQI is not necessarily the lowest unicast CQI.

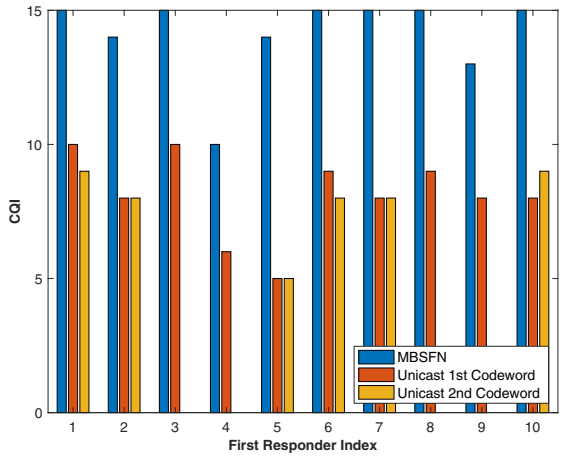

Fig. 8: Comparison between MBSFN CQI and Unicast CQI

The CDF of first responder throughput is shown in Fig. 9, for both unicast and MBSFN. Note that different from Fig. 7, in unicast when spatial multiplexing is triggered and 2 codewords are used for the UE, both codewords contribute to this UE's throughput and together generate one sample in throughput CDF. Meanwhile, in MBSFN 6 out of 10 subframes are used, which is the maximum specified by the standard. It can be observed that the MBSFN CDF is close to a vertical line. This is because of the low target BLER of 0.01, and the fact that all UEs are receiving the same content at the same time, using the same MCS and RBs. Hence all first responders experience similar throughput. In this specific case, MBSFN shows higher throughput. MBSFN also has higher average throughput of 9.76 Mb/s than unicast 6.02 Mb/s, which is not shown in the figure. With increasing number of first responders, this throughput gap will be bigger.

To show the impact of selecting the lowest MCS in MBSFN, the potential throughput UEs would achieve per their individual CQI reporting is plotted in red. This potential throughput is much higher than the actual throughput, and its lowest value is the same as the actual MBSFN throughput. The potential MBSFN throughput is also much higher than the unicast throughput. One reason is the higher effective SNR as shown in Fig. 7. Another reason is that MBSFN uses all RBs for its transmission and that applies to all UEs, while in unicast the RBs are shared by the UEs. That is, the resource used by each UE is much more in MBSFN than that in unicast. However, given the lowest MCS selection in MBSFN, the actual throughput experienced by first responders is much lower than the potential MBSFN throughput.

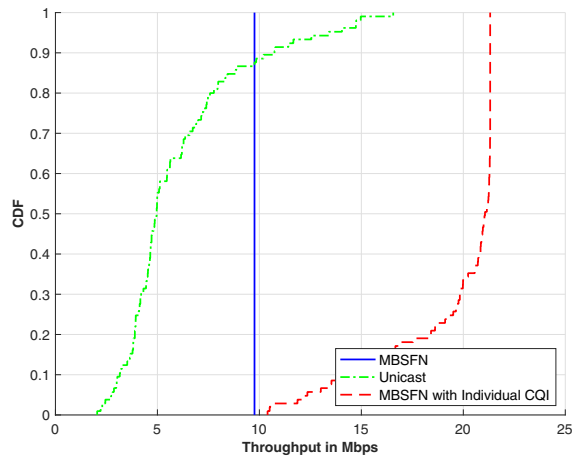

Fig. 9: Throughput CDF for Unicast and MBSFN

Fig. 10 shows the histogram of CQIs for MBSFN reported from all UEs in one TTI. In this case, although majority of the UEs reported the highest possible CQI of 15, there are UEs that reported CQI of 10. These UEs lowered the MCS used by MBSFN, and hence the MBSFN throughput.

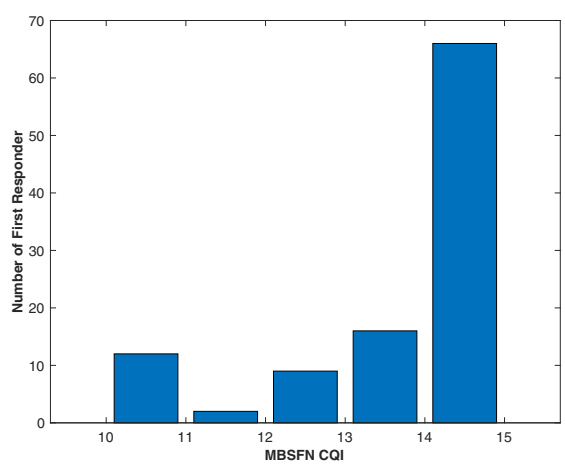

Fig. 10: MBSFN CQI Histogram in TTI 23

Fig. 11 further shows how minimum CQI in MBSFN varies in time. It can be observed that in most time, the minimum

MBSFN CQIs remain stable. The more first responders per sector, the lower the minimum CQI is.

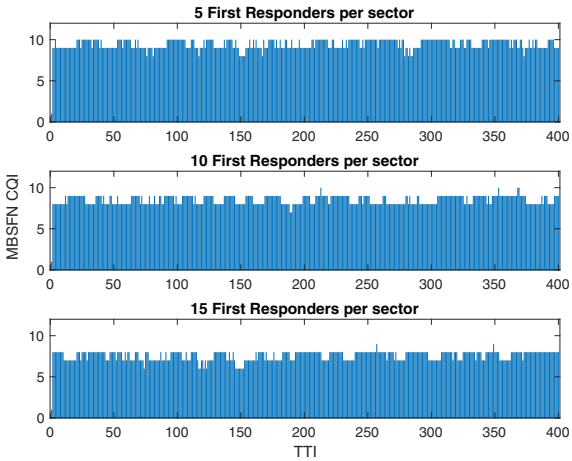

Fig. 11: MBSFN Minimum CQI with Time

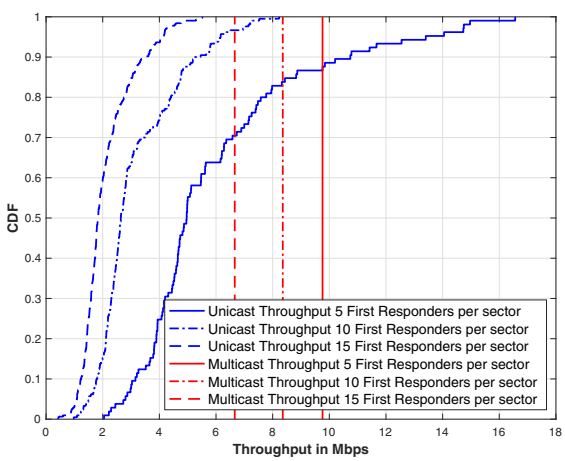

Fig. 12: Throughput CDF with 5, 10, and 15 First Responders per Sector

Finally, Fig. 12 shows first responders' throughput CDF when there are 5, 10, and 15 first responders per sector, respectively. It can be observed that the first responders' throughput in unicast decreases significantly as first responders' density increases, while in MBSFN it is less sensitive. The relatively lower throughput in MBSFN with more first responders is due to the slightly lower MBSFN CQI, as shown in Fig. 11. Also note that in the cases shown, MBSFN throughput is higher than majority of unicast throughput. In case of 15 first responders per sector, the MBSFN throughput is even higher than the highest throughput in unicast. This is consistent with our analysis in Fig. 7.

V. Conclusion

In this paper we generated high fidelity BLER curves for both MBSFN and unicast, and extracted and analyzed SNR points to switch CQIs. The BLER curves and CQI switching points were then fed into our comprehensive system level simulations, which considers unicast with MIMO and MBSFN without MIMO as well as all 3GPP PHY and MAC features. The resulting SINR, throughput, and CQI for both unicast and multicast were also analyzed.

While throughput is one major metric for performance, another perspective of group traffic is that the content is available to first responders simultaneously. Our next step is to introduce other metrics in addition to throughput, and to use the results in this paper to further investigate the trade offs between unicast and multicast. We will also optimize LTE system to meet first responder needs and to ensure quality service for everyone.

References

[1] FirstNet. https://firstnet.gov/content/firstnet-building-nationwide-public-safety-network.

[2] "Minnesota Department of Public Safety Public Safety Wireless Data Network Requirements Project Needs Assessment Report," Minnesota PSN, Tech. Rep., May, 2011.

[3] 3GPP TS36.300, "Evolved Universal Terrestrial Radio Access (E-UTRA) and Evolved Universal Terrestrial Radio Access Network (E-UTRAN); Overall description; Stage 2," 3GPP, Standard.

[4] A. Alexiou, C. Bouras, V. Kokkinos, A. Papazois, and G. Tsichritzis, "Modulation and Coding Scheme Selection in Multimedia Broadcast over a Single Frequency Network Enabled Long Term Evolution Networks," *International Journal of Communication Systems*, vol. 25, 12 2012.

[5] A. Daher, M. Coupechoux, P. Godlewski, P. Ngouat, and P. Minot, "SC-PTM or MBSFN for Mission Critical Communications?" in *2017 IEEE 85th Vehicular Technology Conference (VTC Spring)*, June 2017, pp. 1–6.

[6] J. Chen, M. Chiang, J. Erman, G. Li, K. K. Ramakrishnan, and R. K. Sinha, "Fair and Optimal Resource Allocation for LTE Multicast (eMBMS): Group Partitioning and Dynamics," in *2015 IEEE Conference on Computer Communications (INFOCOM)*, April 2015, pp. 1266–1274.

[7] S. Mitrofanov, A. Anisimov, and A. Turlikov, "eMBMS LTE Usage to Deliver Mobile Data," in *2014 6th International Congress on Ultra Modern Telecommunications and Control Systems and Workshops (ICUMT)*, Oct 2014, pp. 60–65.

[8] 3GPP TS36.213, "Evolved Universal Terrestrial Radio Access (E-UTRA); Physical Layer Procedures," 3GPP, Standard, Jan. 2019.

[9] 3GPP TS36.211, "Evolved Universal Terrestrial Radio Access (E-UTRA); Physical channels and modulation," 3GPP, Standard, Dec. 2018.

[10] M. Rupp, S. Schwarz, and M. Taranetz, *The Vienna LTE-Advanced Simulators: Up and Downlink, Link and System Level Simulation*, 1st ed. Springer Publishing Company, Incorporated, 2016.

[11] "Evaluation Methodology Document (EMD)," IEEE 80216m, Tech. Rep., July 2008.

[12] S. Schwarz and M. Rupp, "Throughput Maximizing Feedback for MIMO OFDM Based Wireless Communication Systems," in *2011 IEEE 12th International Workshop on Signal Processing Advances in Wireless Communications*, June 2011, pp. 316–320.

[13] C. Liu, C. Shen, J. Chuang, R. A. Rouil, and H. A. Choi, "Evaluating unicast and MBSFN in public safety networks," 2019 forthcoming.

[14] L. Rong, O. B. Haddada, and S. Elayoubi, "Analytical Analysis of the Coverage of a MBSFN OFDMA Network," in *IEEE GLOBECOM 2008 - 2008 IEEE Global Telecommunications Conference*, Nov 2008.

[15] 3GPP TS36.212, "Evolved Universal Terrestrial Radio Access (E-UTRA); Multiplexing and Channel Coding," 3GPP, Standard, Jan. 2019.

[16] 3GPP TR25.996, "Spatial Channel Model for Multiple Input Multiple Output (MIMO) Simulations," 3GPP, Standard, July 2017.